Magazine of Civil Engineering

ISSN 2712-8172

journal homepage: http://engstroy.spbstu.ru/

Research article

UDC 69

DOI: 10.34910/MCE.134.7

Bending of orthotropic scalene triangle plates: finite difference modeling

M.S. Beketova[1], ***Zh. Nuguzhinov***[2], ***V.I. Travush***[3], ***N.I. Vatin***[4] ✉, ***S.K. Akhmediyev***[1], ***I.A. Kurokhtina***[1], ***R.A. Shagiyeva***[5], ***V.F. Mikhailov***[1], ***O. Khabidolda***[6]

[1] *Abylkas Saginov Karaganda Technical University, Karaganda, Republic of Kazakhstan*

[2] *Kazakhstan Multidisciplinary Institute of Reconstruction and Development Republican State Enterprise on the Right of Economic Use, Karaganda, Republic of Kazakhstan*

[3] *GORPROJECT, Moscow, Russian Federation*

[4] *Peter the Great St. Petersburg Polytechnic University, St. Peterburg, Russian Federation*

[5] *Toraighyrov University, Pavlodar, Republic of Kazakhstan*

[6] *Karaganda University named after E.A. Buketov, Karaganda, Republic of Kazakhstan*

✉ *vatin@mail.ru*

Keywords: orthotropic material, triangular plate, finite difference method, triangular grid, deflections and forces in the middle surface

Abstract. The object of the study is a transversely bent triangular plate made of an orthotropic material, fixed along the edges of the plate, under the action of a uniformly distributed load. The fourth-order differential equilibrium equations with variable orthotropy parameters were used. The equations were approximated by finite differences for a grid of scalene triangles. Such a grid describes well the boundary contour of triangular plates. The boundary conditions for the grid were written taking into account the orthotropy of the plate material. Seven typical finite difference equations were developed taking into account the boundary conditions along three edges of the plate and the presence of three angles of an irregular triangle. A finite difference matrix was obtained. The matrix structure allows calculating a triangular plate at different angles at the base. It is possible to vary the boundary conditions in the form of rigid or hinged support of the triangular plates. The calculation method takes into account the parameters of the orthotropy of the material in two mutually perpendicular planes. The adaptation of the numerical method to the calculation of orthotropic plates of arbitrary shape was described. The relationships for determining the rigidity characteristics of orthotropic materials were given. An algorithm for simple engineering calculation of triangular orthotropic plates was proposed that allowed performing accurate calculations in variant design. The scientific and applied results of the proposed article will find wide application in mechanics of deformable solids in the field of studying two-dimensional thin-walled structures, as well as in calculating plates of complex geometry with non-uniform mechanical characteristics of their materials.

Funding: This research was funded by the Ministry of Science and Higher Education of the Russian Federation within the framework of the state assignment No 075-03-2025-256 dated 16 January 2025, Additional agreement No 075-03-2025-256/1 dated 25 March 2025, FSEG-2025-0008

Citation: Beketova, M.S., Nuguzhinov, Zh., Travush, V.I., Vatin, N.I., Akhmediyev, S.K., Kurokhtina, I.A., Shagiyeva, R.A., Mikhailov, V.F., Khabidolda, O. Bending of orthotropic scalene triangle plates: finite difference modeling. Magazine of Civil Engineering. 2025. 18(2). Article no. 13407. DOI: 10.34910/MCE.134.7

1. Introduction

In various branches of technology (construction, mechanical engineering, aircraft building, and shipbuilding), orthotropic plates are widely used, in which the physical and mechanical characteristics of materials are symmetrical about three mutually perpendicular planes (wood, plywood, reinforced concrete). Many designs also have orthotropic properties, for example, corrugated and ribbed plates. A lot of works are dealing with studying orthotropic plates. Recent works include [1–3].

A study [4] showed that the general anisotropic property and the variable in-plane stiffness property inherent in composites create significant challenges in the static and dynamic analysis of these new types of variable stiffness composite structures. Therefore, it is important to develop mechanical models and calculation methods for composite lamellar-shell structures of variable stiffness to understand their complex mechanical mechanisms and promote their further application in aerospace engineering.

Publications devoted to triangular orthotropic plates appear much less frequently. In one of the first such publications [5], large amplitude oscillations of right triangular anisotropic plates were analyzed based on von Kármán governing equations. Utilizing the Bubnov–Galerkin procedure, a nonlinear second-order differential equation for the unknown time function was drawn. The equation was solved in terms of Jacobian elliptic functions.

Vibration analysis and multi-objective optimization of stiffened triangular plate was done in [6]. The triangular plate included stiffeners (ribs), which were parallel to each other and parallel to one edge of the triangle. The governing equation of transversal deflection of the plate was obtained by considering the effects of orthotropic characteristics and external excitation. The ordinary differential equation for the system's time response was obtained using the Bubnov–Galerkin method. In the next step, a multi-objective optimization was carried out considering two conflicting objective functions, i.e., maximizing the system's nonlinearity and minimizing the amplitude of vibration. Four decision variables were considered, including the plate's thickness, geometry, and the distance of the stiffeners. Finally, the effects of different parameters on the optimal solutions and the distribution of decision variables were investigated.

The buckling analysis of general triangular anisotropic plates with different boundary conditions subjected to combined in-plane loads was considered in [7, 8]. Solutions for plate buckling were obtained using the Rayleigh–Ritz method combined with a variational formulation. The numerical results were obtained for various triangular geometries with isotropic and anisotropic material properties. The effect of transverse-shear deformation was studied for different triangular geometries. The results confirm the importance of including the effect of transverse-shear deformation in the buckling analysis of composite plates. These results were later used in [9, 10] for optimal design of composite grid-stiffened aircraft panels subjected to global and local buckling constraints. The local buckling of aircraft skin segments is assessed with material anisotropy and transverse shear flexibility. The local buckling of stiffener segments was also assessed.

An accurate and simplified solution was provided in [11] for the free vibration problem of simply supported thin general triangular plates. The proposed method applies to thin plates with linear boundaries regardless of their geometrical shapes. The results were compared with previously published data for the isosceles and general triangles. Good agreements were reported. Although the paper deals only with simple support conditions, the article claims that any combination of classical boundary conditions, with or without complicating factors, can be handled.

The *p*-Ritz method operates with mathematically complete two-dimensional polynomial functions, and boundary polynomial equations raised to appropriate powers are used to approximate the displacements. In the [12], the *p*-Ritz method was used to derive the governing eigenvalue equation for the buckling behavior of triangular plates with both translational and rotational elastic edge constraints. The effect of elastic edge supports on the buckling factors for triangular plates of various vertex angles (aspect ratios) and boundary conditions was examined. The buckling solutions for isosceles and right-angled triangular plates with elastic edge constraints were presented.

The unilateral buckling behavior of point-restrained triangular plates was studied in [13]. The Rayleigh–Ritz method with polynomial-based shape functions was used to study the unilateral buckling behavior of triangular plates with various loading combinations, aspect ratios, boundary conditions, and point restraint configurations. Polynomials and tensionless foundation modeled the displacement functions and restraining medium, respectively. The results were obtained for different boundary conditions, aspect ratios, and various in-plane compressive and shear loadings. Convergence and comparison studies were undertaken to confirm the validity and precision of the solution method.

Free and forced multi-frequency vibrations of stiffened triangular plate with the stiffeners were studied in [14]. The governing motion equation for a triangular plate was developed based on the von Kármán theory. The nonlinear ordinary differential equation of the system using the Bubnov–Galerkin approach was

obtained. Closed-form expressions for the free undamped and large-amplitude vibration of an orthotropic triangular elastic plate were presented using two analytical methods, namely, the energy balance method [15] and the variation approach. It was demonstrated that those two methods were straightforward and reliable techniques for solving those nonlinear differential equations.

A nonlinear vibration of a triangular shape plate with several stiffeners was studied in [16]. The Bubnov–Galerkin method was used to obtain the ordinary differential equation for the system time response. A genetic-based multi-objective optimization was performed to find the geometry and locations of the plate stiffeners.

Three-dimensional structures in the form of triangular plates of thin and medium thickness with homogeneous and inhomogeneous characteristics of materials (isotropic and orthotropic) were considered in [17]. The finite difference method was applied using a grid of scalene triangles as a resolving method. Based on a numerical algorithm and the author's Fortran programs, the leading parameters were obtained from transverse and in-plane loads under various boundary conditions (in bending, buckling, and free oscillations).

In [18], free vibration characteristics of moderately thick composite materials triangular plates under multi-points support boundary conditions were analyzed. An improved Fourier series method was used. Energy equations were established based on the first-order shear deformation theory. The Rayleigh–Ritz technique was adopted to solve unknown coefficients of energy equations with the multi-point support boundary conditions. This study was aimed to simulate real engineering structures with multi-point support. It was shown that the method has a higher accuracy than the finite element method.

In-plane vibration of arbitrary laminated triangular plates with elastic boundary conditions was studied in [19] by the Chebyshev–Ritz method. The coordinate transformation mapped the arbitrarily shaped triangular laminated plate into a square plate to facilitate energy calculation. The displacement functions of the square plate after transformation were expressed as two-dimensional Chebyshev polynomials multiplied by coefficients. The arbitrary elastic boundary conditions of the plate were obtained by changing the stiffness values of each spring with artificial virtual spring technology. The in-plane free vibration characteristics of the triangular laminated plate under different boundary conditions were calculated. The accuracy of this method was verified by comparing with finite element results and experimental results. The comparison shows that the present method has good convergence and satisfactory actuarial accuracy.

The bending of cantilever triangular plates at the same inclination angles of the side edges to the base was investigated in [20]. The finite difference method was applied. Combining the results was applied to solve the problem of an acute angle at the top of the plate. The results of calculating a cantilever bar of variable bending stiffness were combined with similar results of calculating a triangular plate supported along the contour using a reduction factor. This study theoretical provisions and applied results could be partially used to investigate the bending of orthotropic scalene triangle plates supported along the edges.

The frequency and mode of free vibrations of thin isotropic triangular plates with a central hole for different boundary conditions were investigated in [21]. The finite element method was used. Some plates topology of vibration modes was compared to square plates with hinged and clamped edges. The numerical values of the natural frequencies and modes of triangular plates are in good agreement with the experimental results.

The simplistic superposition method was used for analytic free vibration solutions of right triangular plates [22]. The problem was solved by dividing it into three subproblems that were solved by the symplectic techniques via imposing the variable separation on the Hamiltonian-system-based governing equation and symplectic eigen expansion. Then, the analytic frequency and mode shape solutions were obtained by requiring the equivalence between the original problem and the superposition. The comparison with the numerical results for the right triangular plates confirmed the approach's convergence and accuracy.

In this case, the aim of this work is to develop and apply a rarely used and complex type of triangular grid of the finite difference method to plates of complex geometry, in particular for calculating the stress-strain state of triangular orthotropic plates with unequal values of angles at their vertices that has previously been insufficiently studied.

The objective of the study is to evaluate the stress-strain state of triangular orthotropic plates with different boundary conditions under different types of loads, to determine the dependence of the effect of the orthotropy coefficients of boundary conditions, the values of angles at the base on the strength parameters of the bearing capacity of triangular plates.

2. Methods

The object of the study is a transversely bent triangular plate made of orthotropic material, fixed along the edges of the plate, under the action of a uniformly distributed load. Fig. 1 shows the computational scheme of the triangular plate.

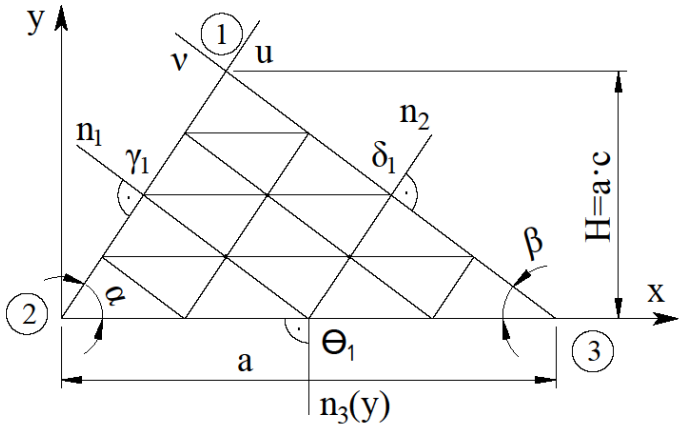

Figure 1. Computational scheme of the triangular plate.

The plate configuration is determined by three parameters: a is the base of the triangle (plate); α, β are the angles of inclination of the side edges to the base (in the general case, α is not equal to β). The study used the well-known initial differential equation for the bending of orthotropic plates [23–25], which has the form:

$$D_1 \frac{\partial^4 w}{\partial x^4} + 2D_3 \frac{\partial^4 w}{\partial x^2 \partial y^2} + 2D_2 \frac{\partial^4 w}{\partial y^4} = q, \tag{1}$$

where $w = w(x, y)$ is the sought deflection function; q is the intensity of the stationary transverse distributed load in the plane of the plate; D_1, D_2, D_3, D_k is the bending and torsional rigidity of the orthotropic material; x, y are the Cartesian coordinates.

The bending and torsional rigidity of the orthotropic material is determined as follows:

$$D_1 = \frac{E_1 t^3}{12(1-\nu_1\nu_2)};\ D_2 = \frac{E_2 t^3}{12(1-\nu_1\nu_2)};$$
$$D_3 = D_1 \cdot \nu_2 + 2D_k;\ D_k = \frac{Gt^3}{12}. \tag{2}$$

Here, E_1, E_2 is the modulus of elasticity of the material in two mutually perpendicular planes; ν_1, ν_2 are Poisson ratios in two mutually perpendicular planes; G is the shear modulus; D_k is the torsional bending rigidity; t is the thickness of the plate.

Then, the orthotropy coefficients were introduced:

$$\alpha_0 = \frac{2 \cdot D_3}{D_1},\ \beta_0 = \frac{D_2}{D_1}. \tag{3}$$

Equation (1), taking into account the accepted designations of (2) and (3), has the form:

$$\frac{\partial^4 w}{\partial x^4} + 2\alpha_0 \frac{\partial^4 w}{\partial x^2 \partial y^2} + \beta_0 \frac{\partial^4 w}{\partial y^4} = \frac{q}{D_1}. \tag{4}$$

Bending moments M_x, M_y and torsional moment M_{xy}, taking into account the structure material orthotropy, have the form:

$$M_x = -D_1\left(\nu_2\frac{\partial^2 w}{\partial y^2}+\alpha_0\frac{\partial^2 w}{\partial x^2}\right);\ M_y = -D_1\left(\nu_1\frac{\partial^2 w}{\partial x^2}+\beta_0\frac{\partial^2 w}{\partial y^2}\right);$$
$$M_{xy} = -D_k\frac{\partial^2 w}{\partial x\partial y}. \tag{5}$$

The boundary conditions of plates supported at the edges are written in the same way as for bending isotropic plates (with hinged or rigidly fixed plate edges):

$$w_i = 0;\ M_{n_j} = 0;\ \partial w_i/\partial n_j = 0, \tag{6}$$

where j in the edge number, n_j is the normal direction to the corresponding plate edges, M_{n_j} is the bending moment in the normal direction.

3. Results and Discussion

It is known that the finite difference method can be a preferred choice for problems on a uniform grid. To apply equation (4) to the bending analysis of a triangular orthotropic plate (Fig. 1), the finite difference method with a grid of scalene triangles is used. The grid of scalene triangles fits well into the oblique contour of the triangular plates. Fig. 2 shows a fragment of the grid of scalene triangles.

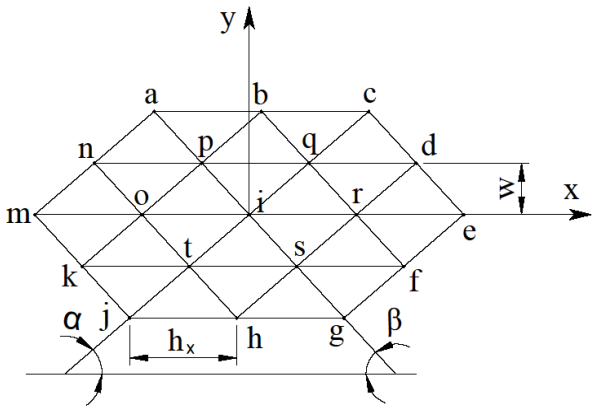

Figure 2. A grid fragment of scalene triangles.

To the i-th node of the grid of scalene triangles, equation (4) will have the form (without taking into account the boundary conditions) that is presented in work [17]:

$$\psi_1 w_i + \psi_2\left(w_o + w_r\right) + \psi_3\left(w_P + w_{1S}\right) + \psi_4\left(w_q + w_t\right) +$$
$$+\psi_5\left(w_n + w_f\right) + \psi_6\left(w_b + w_h\right) + \psi_7\left(w_d + w_k\right) + \psi_8\left(w_m + w_e\right) + \tag{7}$$
$$+\psi_9\left(w_a + w_g\right) + \psi_{10}\left(w_c + w_j\right) = \frac{qhy^4}{D_1}.$$

Here, the grid parameters ψ_1, ψ_2, ψ_3, ψ_4, ψ_5, ψ_6, ψ_7, ψ_8, ψ_9, ψ_{10} are determined in such a way:

$$\psi_1 = 6C^4 + \alpha_0 C^2\left(-6AB+4\right) + \beta_0\left[4\left(AB-1\right)^2 + 2\left(AB\right)^2 + 2A^2 + 2B^2\right];$$
$$\psi_2 = -4C^4 + \alpha_0 C^2\left(4AB-2\right) + \beta_0\left[-4AB\left(AB-1\right) + 2AB\right];$$
$$\psi_3 = \alpha_0 C^2\left(B-2A\right) + \beta_0\left[4A\left(AB-1\right) - 2A^2B\right];\ \psi_5 = \alpha_0 C^2 + 2\beta_0 A^2 B; \tag{8}$$
$$\psi_6 = 2\beta_0 AB;\ \psi_7 = \alpha_0 C^2 B - 2\beta_0 AB^2;\ \psi_8 = C^4 - \alpha_0 C^2 AB + \beta_0\left(AB\right)^2;$$
$$\psi_9 = \beta_0 A^2;\ \psi_{10} = \beta_0 B^2.$$

The angles α and β define the parameters A, B, C and U:

$$A=\frac{\sin\beta\cos\alpha}{\sin(\alpha+\beta)};\ B=\frac{\sin\alpha\cos\beta}{\sin(\alpha+\beta)};\ C=\frac{\sin\alpha\sin\beta}{\sin(\alpha+\beta)};$$
$$U=C^2-AB. \tag{9}$$

The equation in the particular case for an isotropic plate for the i-th grid node is also written according to [17] in the following form:

$$\varphi_1 w_1+\varphi_2(w_o+w_r)+\varphi_3(w_p+w_s)+\varphi_4(w_q+w_t)+$$
$$+\varphi_5(w_n+w_f)+\varphi_6(w_b+w_h)+\varphi_7(w_d+w_k)+\varphi_8(w_m+w_e)+ \tag{10}$$
$$+\varphi_9(w_a+w_g)+\varphi_{10}(w_c+w_j)=\frac{qhy^4}{D_1},$$

where

$$\varphi_1=2\left[2(U+1)^2+A^2+B^2+U^2\right];\ \varphi_2=-2\left[2U(U+1)-AB\right];$$
$$\varphi_3=-2\left[2A(U+1)-BU\right];\ \varphi_4=-2\left[2B(U+1)-AU\right]; \tag{11}$$
$$\varphi_5=2AU;\ \varphi_6=2AB;\ \varphi_7=2BU;\ \varphi_8=U^2;\ \varphi_9=A^2;\ \varphi_{10}=B^2.$$

Thus, equations (7), (10) differ only in expressions (8), (11), respectively.

The original equation (1) must be accompanied by the corresponding boundary conditions at the edges of the plate. For continuously supported sides of the plate along the perimeter (Fig. 1), the boundary conditions are as follows:

$$w_i=0;\ \partial w_i/\partial n_j=0;\ \partial^2 w_i/\partial n_j^2=0, \tag{12}$$

where w_i is the deflection at the i-th node of the plate contour; n_j are the normals to the edges of the plate (Fig. 1); j =1, 2 are the numbers of the plate edges.

Boundary conditions (11) for the i-th grid node are written in the finite differences in the group form as follows:

- For the left edge of the plate (Fig. 3, a):

$$w_q=w_i=w_t=0;\ (\psi_8 w_0+0.5\psi_7 w_p)=\gamma_1(\psi_8 w_r+0.5\psi_7 w_S); \tag{13}$$

- For the right edge of the plate (Fig. 3, b):

$$w_q=w_i=w_S=0;\ (\psi_8 w_r+0.5\psi_5 w_q)=\delta_1(\psi_8 w_o+0.5\psi_5 w_t); \tag{14}$$

- For the plate base (Fig. 3, c):

$$w_o=w_i=w_r=0;\ (0.5\psi_7 w_s+0.5\psi_5 w_t)=\theta_1(0.5\psi_7 w_p+0.5\psi_5 w_t). \tag{15}$$

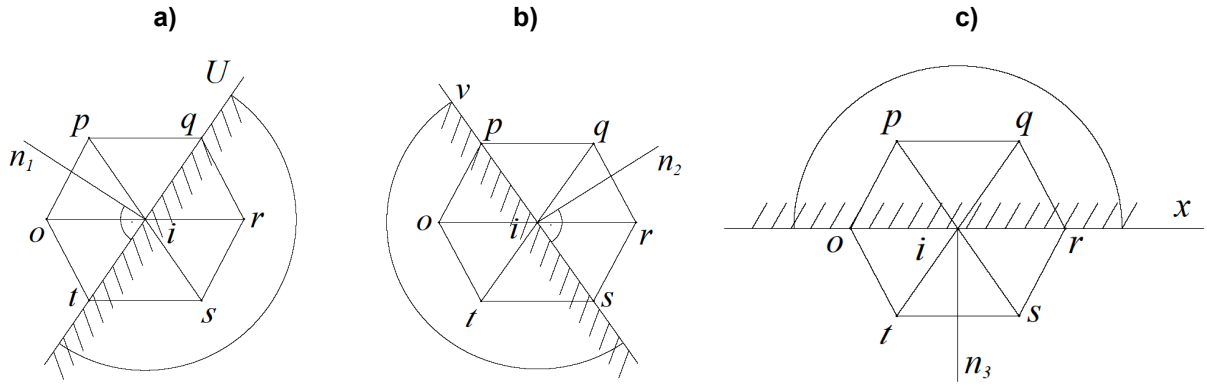

Figure 3. Definition of boundary conditions: a) the left edge of the plate "1-2"; b) the right edge of the plate "1-3"; c) the base of the plate "2-3".

The coefficients in expressions (13)–(15) took the following values: $(\gamma_1 = \delta_1 = \theta_1) = -0.1$ for hinge-support edges of the plate; $(\gamma_1 = \delta_1 = \theta_1) = +1.0$ for rigid edges of the plate.

Boundary conditions (13)–(15) modify the basic finite difference equation for orthotropic triangular plates (7) taking into account and takes the form of seven typical finite difference equations for seven characteristic grid nodes. Fig. 4 illustrates the numbering of typical grid equations.

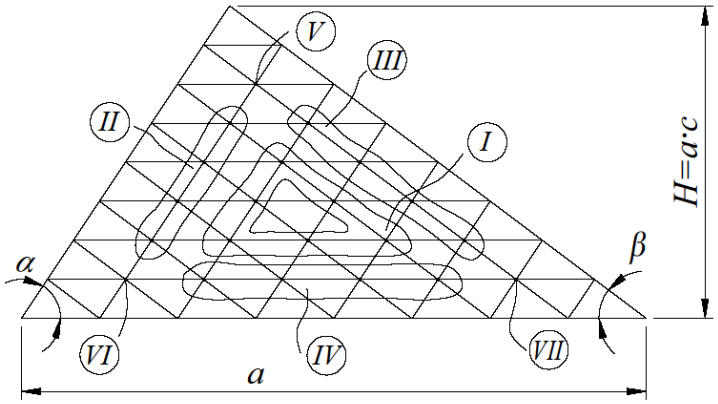

Figure 4. Numbering of typical grid equations.

With the triangular plate discretized into N grid divisions and continuous edge support along the perimeter, 21 calculation (intra-contour) nodes were obtained. Fig. 5 shows the numbering of some calculation nodes.

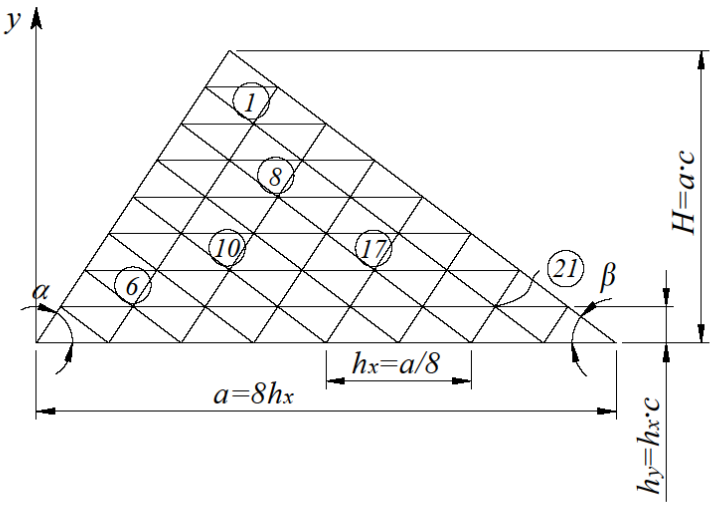

Figure 5. Numbering of the analysis nodes of the triangular grid.

The finite difference equations for all 21 computational nodes of the triangular grid (Fig. 5) constitute a system of linear algebraic equations of the 21st order, which in matrix form has the form:

$$\mathbf{D}_u \cdot \vec{\mathbf{w}} = \vec{\mathbf{P}}. \tag{16}$$

Here, $\mathbf{D}_u$ is a square matrix of the 21st order; $\vec{\mathbf{w}} = \left|\{w_1,\ w_2,\ \ldots,\ w_{21}\}\right|$ is the vector of the sought deflections; $\vec{\mathbf{P}} = \left|\{P_1,\ P_2,\ \ldots,\ P_{21}\}\right|$ is the vector of free terms, taking into account the transverse load acting on the surface.

With uniform distribution of the intensity of the transverse distributed load q over the plate, there is:

$$P_i = qh_y^4 \big/ D_1, \tag{17}$$

where D_1 is accepted based on expression (3); $h_y = AC/8$ is a grid step along the y axis (Fig. 5).

Thus, the algorithm for calculating orthotropic plates proposed by the authors consists of applying expressions (2), (3), (7)–(9), (13)–(15) to implement equation (16).

Using the SMath Studio program [26, 27], a number of research problems were solved based on expression (16). There was studied the effect of the following:

- the type of boundary conditions (using the $\gamma_1,\ \delta_1,\ \theta_1$ coefficients);
- the plate geometry (setting the values of angles α and β at the base of the plate);
- the orthotropy coefficients α_0 and β_0 determined by formula (3), on the value of nodal deflections $\left(w_i = 1,\ 2,\ \ldots,\ 21\right)$.

Figs. 6 and 7 show the graphical dependencies of the deflections at the grid nodes δ = 1, 6, 8, 10, 17, 21 (Fig. 5) for equilateral $\left(\alpha = \beta = 60^\circ\right)$ triangular orthotropic plates (with α_0 = 0.66; 1; 1.5; 2.0 and β_0 = 0.5; 1; 1.5; 2.0) with rigid and hinged edges with the number of grid divisions $N = 8$.

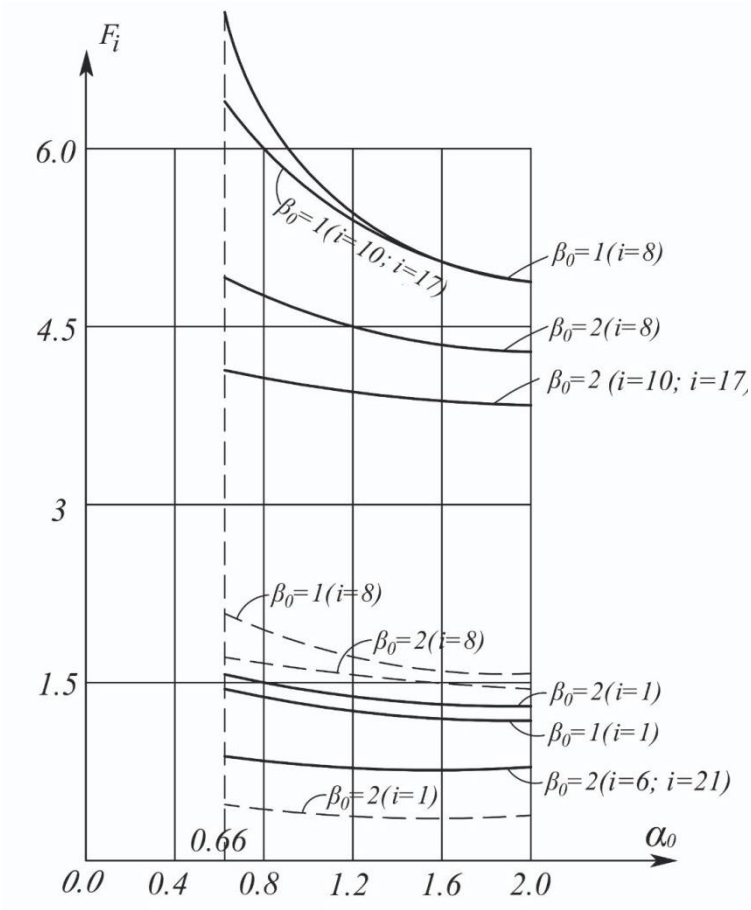

____ – hinged support of the plate edges, _ _ _ – rigid support of the plate edges

Figure 6. Dependence of deflections at the nodes (i = 1, 8, 10, 17) of triangular orthotropic plates with changing the orthotropy coefficients α_0.

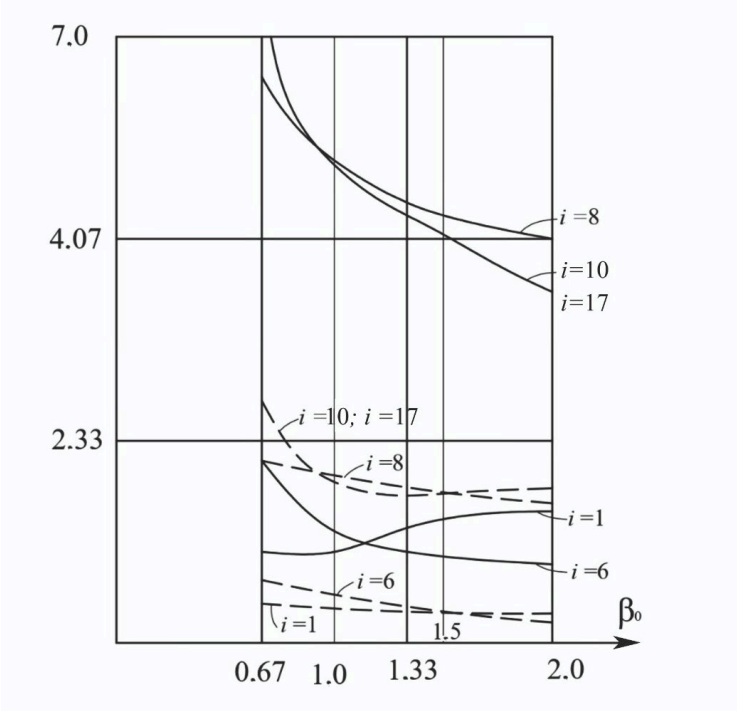

_____ – hinged support of the plate edges, _ _ _ – rigid support of the plate edges.

Figure 7. Dependence of deflections at nodes (i = 1, 8, 10, 17) of triangular orthotropic plates on the orthotropy coefficient β_0 with a constant orthotropy coefficient α_0 = 1.

Tables 1 and 2 present the results of numerical calculations of equilateral triangular plates with different edge fastening methods.

Table 1. Deflections of nodes under different boundary conditions and orthotropy coefficients.

Support type	β_0	α_0	Deflections $\left(w_i \cdot 10^4 \frac{D_1}{qa^4}\right)$ of nodes					
			1	**6**	**21**	**8**	**10**	**17**
Hinged support around the perimeter, $\alpha = \beta = 60^0$, $N = 8$	2	0.66	1.537	0.97	0.97	4.97	4.29	4.29
		1	1.44	0.92	0.92	4.68	4.07	4.07
		2	1.21	0.8	0.8	4.0	3.55	3.55
	1	0.66	1.45	1.58	1.58	6.36	6.21	6.21
		1	1.38	1.46	1.46	5.87	5.78	5.78
		1.5	1.288	1.317	1.317	5.28	5.25	5.25
	Isotropic material	2	1.202	1.202	1.202	4.807	4.807	4.807
Rigid support around the perimeter, $\alpha = \beta = 60^0$, $N = 8$	2	0.66	0.38	0.22	0.22	1.698	1.33	1.33
		1	0.36	0.21	0.21	1.62	1.29	1.29
		2	0.31	0.18	0.18	1.42	1.17	1.17
	1	0.66	0.35	0.36	0.36	2.1	1.99	1.99
		1	0.33	0.34	0.34	1.98	1.9	1.9
		1.5	0.308	0.309	0.309	1.82	1.78	1.78
	Isotropic material	2	0.29	0.29	0.29	1.68	1.68	1.68

Table 2. Deflections of nodes under different boundary conditions and orthotropy coefficient β_0 and constant orthotropy coefficient α_0.

	β_0	α_0	Deflections $\left(w_i \cdot 10^4 \frac{D_1}{qa^4}\right)$ of nodes					
			1	**6**	**21**	**8**	**10**	**17**
Hinged support around the perimeter, $\alpha = \beta = 60^0$, $N = 8$	0.5	1	1.28	2.14	2.14	6.83	7.7	7.79
	1		1.38	1.46	1.46	5.87	5.78	5.78
	1.5		1.43	1.125	1.125	5.19	4.74	4.74
	2		1.44	0.92	0.92	4.68	4.07	4.07
Rigid support around the perimeter, $\alpha = \beta = 60^0$, $N = 8$	0.5	1	0.3	0.5	0.5	2.21	2.63	2.63
	1		0.33	0.34	0.34	1.98	1.9	1.94
	1.5		0.35	0.257	0.257	1.777	1.526	4.526
	2		0.361	0.21	0.21	1.617	1.289	1.289

Based on the data of Tables 1 and 2, there can be concluded the following:

- with increasing the orthotropy coefficient α_0 (Fig. 6) for different β_0 and different boundary conditions, the deflections in the calculated nodes decrease monotonically;
- with increasing the orthotropy coefficient β_0 (Fig. 7) for constant values $\left(\alpha_0 = 1 \approx \text{const}\right)$, the deflections in the plate nodes change according to a complex relationship;
- for an equilateral isotropic triangular plate $\left(\alpha_0 = 2,\ \beta_0 = 1\right)$, there are three axes of symmetry along its three medians. In this case, there is equality of deflections in nodes 1, 6, and 21;

- for equilateral orthotropic triangular plates, there is only one axis of elastic symmetry. This axis of symmetry is the y-axis. In this case, the deflections are equal only in nodes 6 and 21 (Figs. 6 and 7, Tables 1 and 2). To evaluate the grid convergence, this problem was solved for two numbers of partitions of the plate sides – 4, 8. The results were as follows:
- for the number of partitions $N = 4,$ the deflection in the middle of the median of the triangle is 5.96;
- for the number of partitions $N = 8,$ the deflection in the middle of the median of the triangle is 4.97;
- the resulting convergence graph (Fig. 8) was obtained using the Richardson extrapolation formula [28].

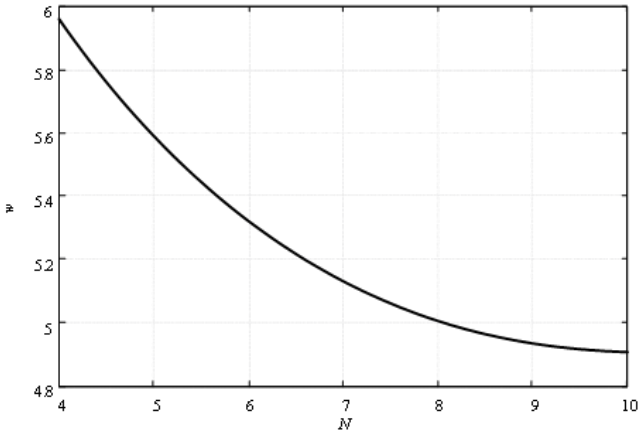

Figure 8. The grid convergence graph.

To assess reliability of the presented results, a finite element calculation was performed for an equilateral triangular plate with a hinged support along the perimeter in order to determine the deflection at node 8 (Fig. 5), if E_1 = 1.5·10^{11} Pa, E_2 = 1.0·10^{11} Pa, ν_1 = 0.1, ν_2 = 0.2, t = 2.5·10^{-3} m, q = 1.0 kPa. The following value of u = 2.584·10^{-3} m was obtained. When switching to dimensionless coefficients, the deflection at node at α_0 = 0.66, β_0 = 2, is as follows:

$$w_8 = \frac{D_1 \cdot u}{q \cdot a^4} \cdot 10^4 = 5.15.$$

The error with the tabular value (Table 1) is $\delta = \left(5.15 - 4.97\right) / 4.97 \cdot 100\% = 3.6\%,$ which indicates the acceptable accuracy of the described calculation algorithm based on the finite difference method.

It was found that when the values of the orthotropy coefficients approach the values of α_0 = 2 and β_0 = 1, the orthotropy factor of materials can be neglected in the calculations.

To assess the reliability of the presented results, an alternative calculation by the finite element method in the ANSYS program was performed for an orthotropic equilateral triangular plate with hinged support along the perimeter in order to determine the deflection in the vicinity of the node (i = 8) (Fig. 11) E_1 = 1.5·10^{11} Pa, E_2 = 1.0·10^{11} Pa, ν_1 = 0.1, ν_2 = 0.2, t = 2.5·10^{-3} m, q = 1.0 kPa. In this case, the following value of u = 2.403·10^{-3} m was obtained.

To verify the reliability of the presented results, an alternative finite element analysis was performed in ANSYS to determine the deflection of an orthotropic equilateral triangular plate with hinged supports along its perimeter. The hinged support was in the vicinity of the node (i = 8) with E_1 = 1.5·10^{11} Pa, E_2 = 1.0·10^{11} Pa, ν_1 = 0.1, ν_2 = 0.2, t = 2.5·10^{-3} m, q = 1.0 kPa (Fig. 11). In this case, the following value of u = 2.403·10^{-3} m was obtained.

When switching to dimensionless coefficients, the deflection in the $\alpha_0 = 0.66$ node with $\beta_0 = 2,$ is as follows:

$$w_8 = \frac{D_1 \cdot u}{q \cdot a^4} \cdot 10^4 = 4.789.$$

The error with the tabular value (Table 1) is $\delta = \left(4.97 - 4.789\right) / 4.789 \cdot 100\% = 3.8\%,$ which indicates the acceptable accuracy of the calculation algorithm based on the finite difference method proposed by the authors of the article.

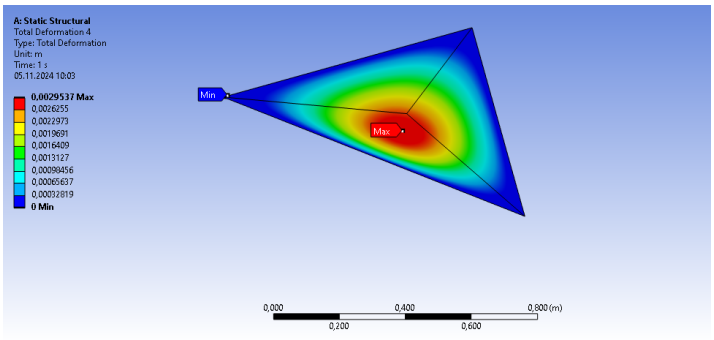

Figure 8. Isolines of deflections of a triangular orthotropic plate under a uniformly distributed load with hinged support of the edges.

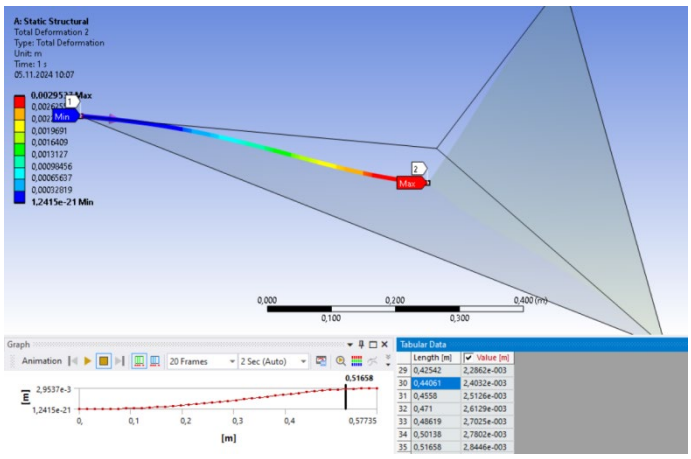

Figure 9. Diagram of deflections in the directions of the median AB.

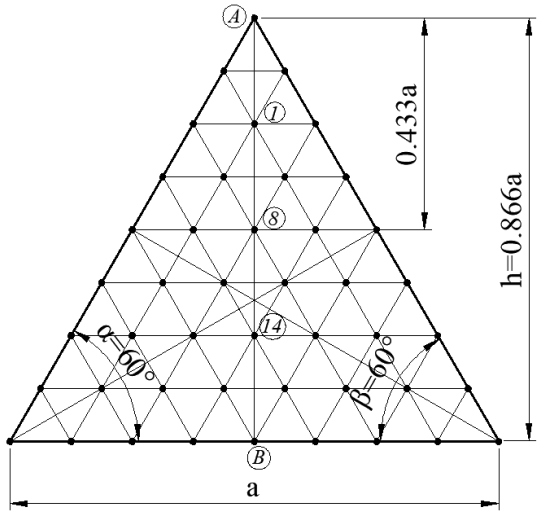

Figure 10. Computational scheme of an orthotropic equilateral plate.

4. Conclusion

The object of the study is a transversely bent triangular plate made of orthotropic material, fixed along the edges of the plate, under the action of a uniformly distributed load. An algorithm for a simple engineering calculation of triangular orthotropic plates based on the finite difference method is given, which allows performing manual or machine calculations with sufficient accuracy in variant (or sketch) design. At the same time, the technical problem of boundary conditions for the edges of triangular plates is solved in the form of the idea of paired exclusion of deflections of contour nodes, which occurs when using a grid of scalene triangles; when using a known rectangular grid, such a problem does not arise.

In the proposed research method, the original differential equations of the 4th order with variable orthotropy coefficients based on finite difference approximation are replaced by grid equations using a grid of scalene triangles. As a result, a mathematical transition occurs to a system of linear algebraic equations, the solution of which results in deflections at the nodes of the applied grid, and then the corresponding internal forces are calculated.

The results obtained allow drawing the following conclusions.

1. The main and typical finite difference equations for a grid of scalene triangles (Fig. 2) are obtained, taking into account changes in the parameters of the plate geometry (angles α and β), boundary conditions (coefficients $\gamma_1,\ \delta_1,\ \theta_1$), material orthotropy (coefficients $\alpha_0,\ \beta_0$), and the number of grid partitions N.
2. The boundary conditions for a grid of scalene triangles are written in an original group (pair) form, which allows us to take into account the presence of oblique edges of irregular (not equilateral) triangular plates;
3. Calculation of the deflection of equilateral $\left(\alpha=\beta=60^\circ\right)$ orthotropic triangular plates (equation (16)). The deflection of equilateral $\left(\alpha=\beta=60^\circ\right)$ orthotropic triangular plates was investigated with the number of grid divisions $N=8,$ which ensures sufficient engineering accuracy.
4. An alternative calculation of an orthotropic equilateral triangular plate using the finite element method confirmed the reliability of the numerical calculation algorithm proposed by the authors of this article.
5. The results of this study expand the range of problems to be solved for triangular orthotropic plates with their geometric asymmetry (oblique, scalene plates), which is the basis for further theoretical and practical developments in the field of mechanics of thin-walled structures.

References

1. Eröz, M. Stress analysis of a pre-stretched orthotropic plate with finite dimensions. Transactions of the Canadian Society for Mechanical Engineering. 2021. 45(2). Pp. 346–354. DOI: 10.1139/tcsme-2019-0241
2. Xu, Y., Wu, Z. Exact solutions for rectangular anisotropic plates with four clamped edges. Mechanics of Advanced Materials and Structures. 2022. 29(12). Pp. 1756–1768. DOI: 10.1080/15376494.2020.1838007
3. Yu, Q. A hierarchical wavelet method for nonlinear bending of materially and geometrically anisotropic thin plate. Communications in Nonlinear Science and Numerical Simulation. 2021. 92. Article no. 105498. DOI: 10.1016/j.cnsns.2020.105498
4. Chen, X., Nie, G., Zhong, Z. Research Progress on Static and Dynamic Problems of Variable Angle Tow Composite Plates and Shells. Chinese Quarterly of Mechanics. 2023. 44(1). Pp. 1–14. DOI: 10.15959/j.cnki.0254-0053.2023.01.001
5. Nowinski, J.L., Ismail, I.A. Large oscillations of an anisotropic triangular plate. Journal of the Franklin Institute. 1965. 280(5). Pp. 417–424. DOI: 10.1016/0016-0032(65)90531-4
6. Sathyamoorthy, M. Effects of large amplitude and transverse shear on vibrations of triangular plates. Journal of Sound and Vibration. 1985. 100(3). Pp. 383–391. DOI: 10.1016/0022-460X(85)90294-9
7. Jaunky, N., Knight Jr., N.F., Ambur, D.R. Buckling analysis of general triangular anisotropic plates using polynomials. Collection of Technical Papers – AIAA/ASME/ASCE/AHS/ASC Structures, Structural Dynamics and Materials Conference. 1995. 4. Pp. 2647–2654.
8. Jaunky, Navin, Knight, N.F., Ambur, D.R. Buckling analysis of general triangular anisotropic plates using polynomials. AIAA Journal. 1995. 33(12). Pp. 2414–2417. DOI: 10.2514/3.13000
9. Jaunky, N., Knight Jr., N.F., Ambur, D.R. (). Optimal design of general stiffened composite circular cylinders for global buckling with strength constraints. Composite Structures. 1998. 41(3–4), Pp. 243–252. DOI: 10.1016/S0263-8223(98)00020-8
10. Jaunky, N., Knight Jr. N.F., Ambur, D.R. Optimal design of grid-stiffened composite panels using global and local buckling analyses. 37th AIAA/ASME/ASCE/AHS/ASC Structure, Structural Dynamics and Materials Conference. Salt Lake City UT, 1996. Pp. 2315–2325. DOI: 10.2514/6.1996-1581
11. Saliba, H.T. Free vibration of simply supported general triangular thin plates: An accurate simplified solution. Journal of Sound and Vibration. 1996. 196(1). Pp. 45–57. DOI: 10.1006/jsvi.1996.0466

12. Xiang, Y. Buckling of triangular plates with elastic edge constraints. Acta Mechanica. 2002. 156(1–2). Pp. 63–77. DOI: 10.1007/BF01188742
13. Dayyani, I., Moore, M., Shahidi, A. Unilateral buckling of point-restrained triangular plates. Thin-Walled Structures. 2013. 66. Pp. 1–8. DOI: 10.1016/j.tws.2013.01.007
14. Askari, H., Saadatnia, Z., Esmailzadeh, E., Younesian, D. Multi-frequency excitation of stiffened triangular plates for large amplitude oscillations. Journal of Sound and Vibration. 2014. 333(22). Pp. 5817–5835. DOI: 10.1016/j.jsv.2014.06.026
15. Esmailzadeh, E., Younesian, D., Askari, H. Energy Balance Methods. Solid Mechanics and Its Applications. 2019. 252. Pp. 73–122. DOI: 10.1007/978-94-024-1542-1_3
16. Saadatnia, Z., Rahnamayan, S., Esmailzadeh, E. Vibration Analysis and Multi-Objective Optimization of Stiffened Triangular Plate. Proceedings of the ASME Design Engineering Technical Conference. Buffalo NY, 2014. Article no. V008T11A033. DOI: 10.1115/DETC2014-35553
17. Akhmediev, S.K., Zhakibekov, M.E., Kurokhtina, I.N., Nuguzhinov, Z.S. Numerical study of the stress-strain state of structures such as thin triangular plates and plates of medium thickness. 2015. 2(259). Pp. 28–33.
18. Wang, Q., Xie, F., Liu, T., Qin, B., Yu, H. Free vibration analysis of moderately thick composite materials arbitrary triangular plates under multi-points support boundary conditions. International Journal of Mechanical Sciences. 2020. 184. Article no. 105789. DOI: 10.1016/j.ijmecsci.2020.105789
19. He, D., Liu, T., Qin, B., Wang, Q., Zhai, Z., Shi, D. In-plane modal studies of arbitrary laminated triangular plates with elastic boundary constraints by the Chebyshev-Ritz approach. Composite Structures. 2021. 271. Article no. 114138. DOI: 10.1016/j.compstruct.2021.114138
20. Akhmediyev, S.K., Khabidolda, O., Vatin, N.I., Yessenbayeva, G.A., Muratkhan, R. Physical and Mechanical State of Cantiliver Triangular Plates. Journal of Mathematics, Mechanics and Computer Science. 2023. 118(2). Pp. 64–73. DOI: 10.26577/JMMCS.2023.v118.i2.07
21. Grigorenko, O.Y., Borisenko, M.Y., Boichuk, O.V, Vasil'eva, L.Y. Free Vibrations of Triangular Plates with a Hole. International Applied Mechanics. 2021. 57(5). Pp. 534–542. DOI: 10.1007/s10778-021-01104-3
22. Yang, Y., An, D., Xu, H., Li, P., Wang, B., Li, R. On the symplectic superposition method for analytic free vibration solutions of right triangular plates. Archive of Applied Mechanics. 2021. 91(1). Pp. 187–203. DOI: 10.1007/s00419-020-01763-7
23. Ambartsumian, S.A. On the theory of bending of anisotropic plates and shallow shells. Journal of Applied Mathematics and Mechanics. 1960. 24(2). Pp. 500–514. DOI: 10.1016/0021-8928(60)90052-6
24. Ambartsumian, S.A. Membrane Theory of Plates. Foundations of Engineering Mechanics. Springer. Cham, 2021. Pp. 73–103. DOI: 10.1007/978-3-030-71326-3_4
25. Poniatovskii, V.V. On the theory of bending of anisotropic plates. Journal of Applied Mathematics and Mechanics. 1964. 28(6). Pp. 1247–1254. DOI: 10.1016/0021-8928(64)90036-X
26. Brezinski, C. Some pioneers of extrapolation methods. The Birth of Numerical Analysis. World Scientific Publishing Company, 2009. Pp. 1–22. WORLD SCIENTIFIC. DOI: 10.1142/9789812836267_0001
27. Nuzhdin, L., Mikhailov, V., Rezyapkin, V. Modeling and analysis of the pile cluster foundation in SCAD and SMath Studio. Proceedings of 16th Asian Regional Conference on Soil Mechanics and Geotechnical Engineering (ARC 2019). Taipei, 2020.
28. Zlatev, Z., Dimov, I., Faragó, I., Georgiev, K., Havasi, Á. Stability of the Richardson Extrapolation combined with some implicit Runge–Kutta methods. Journal of Computational and Applied Mathematics. 2017. 310. Pp. 224–240. DOI: 10.1016/j.cam.2016.03.018

Information about the authors:

Moldir Sailaubekovna Beketova,
ORCID: https://orcid.org/0009-0003-2248-312X
E-mail: moldir-9292@mail.ru

Zhmagul Smagulovich Nuguzhinov, *Doctor of Technical Sciences*
ORCID: https://orcid.org/0000-0002-0252-2115
E-mail: kazmirr@mail.ru

Vladimir Ilyich Travush, *Doctor of Technical Sciences*
ORCID: https://orcid.org/0000-0003-1991-7233
E-mail: vtravush@mail.ru

Nikolai Ivanovich Vatin, *Doctor of Technical Sciences*
ORCID: https://orcid.org/0000-0002-1196-8004
E-mail: vatin@mail.ru

Serik Kabultaevich Akhmediyev, *PhD in Technical Sciences*
ORCID: https://orcid.org/0000-0001-6723-4571
E-mail: serik.akhmediyev.50@mail.ru

Irina Alekseevna Kurokhtina,
ORCID: https://orcid.org/0000-0002-8367-7636

E-mail: kurohtina.ira@mail.ru

***Roza Abdullaevna Shagiyeva**, PhD in Technical Sciences*
ORCID: https://orcid.org/0009-0003-1867-7300
E-mail: shagieva2008@mail.ru

***Valentin Feliksovich Mikhailov**, PhD in Technical Sciences*
ORCID: https://orcid.org/0000-0002-2588-9438
E-mail: v.mikhailov@ktu.edu.kz

***Omirkhan Khabidolda**, PhD*
ORCID: https://orcid.org/0000-0001-7909-7201
E-mail: oka-kargtu@mail.ru

Received 14.01.2025. Approved after reviewing 23.03.2025. Accepted 30.03.2025.